The nature of electron lone pairs in $BiVO_4$

D. J. Payne,[1,a)] M. D. M. Robinson,[1] R. G. Egdell,[1] A. Walsh,[2] J. McNulty,[3] K. E. Smith,[3] and L. F. J. Piper[4,b)]
[1]*Department of Chemistry, Chemistry Research Laboratory, University of Oxford, 12 Mansfield Road, Oxford OX1 3TA, United Kingdom*
[2]*Department of Chemistry, Centre for Sustainable Chemical Technologies, University of Bath, Claverton Down, Bath BA2 7AY, United Kingdom*
[3]*Department of Physics, Boston University, 590 Commonwealth Ave., Boston, Massachusetts 02215, USA*
[4]*Department of Physics, Applied Physics and Astronomy, Binghamton University, Binghamton, New York 13902, USA*

(Received 14 April 2011; accepted 30 April 2011; published online 26 May 2011)

The electronic structure of $BiVO_4$ has been studied by x-ray photoelectron, x-ray absorption, and x-ray emission spectroscopies, in comparison with density functional theory calculations. Our results confirm both the direct band gap of 2.48 eV and that the Bi 6*s* electrons hybridize with O 2*p* to form antibonding "lone pair" states at the top of the valence band. The results highlight the suitability of combining s^2 and d^0 cations to produce photoactive ternary oxides. © *2011 American Institute of Physics*. [doi:10.1063/1.3593012]

Photoelectrochemical (PEC) water splitting, based upon the original concept by Honda and Fujishima using UV-light and rutile TiO_2 (Ref. 1) provides a means of storing solar energy in chemical bonds in an analogous way to fossil fuels. Two fundamental differences are first that the "stored sunlight" in fossil fuels develops over a time scale of millions of years, compared to instantaneous fuel generation from PEC water splitting and second, the by product of fossil fuels is predominantly CO_2 (with its associated link to climate change), compared to water from H_2/O_2 fuel. The development of a suitable material to facilitate the efficient PEC generation of H_2/O_2 from the visible part of the solar spectrum is still being sought and until this is achieved the "hydrogen economy" remains beyond the horizon.

Metal oxides are considered the most suitable candidate materials for PEC applications due to their stability in aqueous solutions. Unfortunately they typically exhibit poor spectral match with the water splitting potentials, with large band gaps in the ultraviolet region of the electromagnetic spectrum, as well as low charge carrier mobilities and high electron-hole recombination rates. WO_3 is commonly used, but $BiVO_4$,[2,3] and recently Ag_3PO_4,[4] have displayed superior performance. In the case of monoclinic $BiVO_4$, hybridization between Bi 6*s* states and O 2*p* states at the top of the valence band (VB) has been suggested to be responsible both for the small band gap of 2.5 eV and the high hole mobility.[2] Despite its importance in determining the PEC behavior, few experimental studies of the electronic structure of $BiVO_4$ exist. Recent density functional theory (DFT) calculations by Walsh *et al.*[5] examined the nature of the band gap and the role of the Bi 6*s* electrons in terms of the revised lone pair (RLP) model of Payne *et al.*[6] A direct band gap between the Bi 6*s*–O 2*p* antibonding derived valence band maximum (VBM) and the coupled V 3*d*, O 2*p*, and Bi 6*p* conduction band minimum (CBM) away from the Brillouin zone center. Most importantly, the orbital coupling is expected to produce relatively light and equal hole and electron effective masses (on the order of $0.3m_0$).

Considering the importance of $BiVO_4$ for PEC applications, we have examined the electronic structure using a combination of x-ray photoemission spectroscopy (XPS), x-ray emission spectroscopy (XES), and x-ray absorption spectroscopy (XAS). These techniques provide information regarding the density of states (DOS); with VB-XPS one measures the total DOS while dipole selection rules associated with XES and XAS enables one to extract the element- and orbital-sensitive partial DOS (pDOS). When used in combination, these techniques have: provided insight into the role of 6*s* lone pair compounds, e.g., α-PbO and Bi_2O_3;[6] revised our understanding of the fundamental band gap of In_2O_3;[7] and, experimentally elucidated the electronic structure and vanadium charge state of complicated vanadate systems (e.g., heavily Cr-doped VO_2).[8]

Pure single-phase monoclinic $BiVO_4$ was formed by ceramic solid synthesis, whereby the reactants, Bi_2O_3 (Sigma-Aldrich 99.999%) and V_2O_5 (Sigma-Aldrich 99.99%), were ground in stoichiometric quantities in an agate mortar, pelletized between tungsten carbide dies under 5 ton for 5 min and then fired at 600 °C for 16 h. The products were reground and refired at 900 °C for an additional 16 h. X-ray diffraction patterns (not shown) of the end product confirmed a phase-pure monoclinic solid had been prepared. The optical band gap of the monoclinic $BiVO_4$ was measured by diffuse reflectance spectroscopy using an MgO standard. The data are presented in terms of a plot of $[F(R)h\nu]^2$ versus photon energy, where $F(R)$ is the Kubelka–Munk function. Figure 1(a) displays the results for monoclinic $BiVO_4$ that are consistent with a direct band gap of 2.48 eV. This is in agreement with UV-visible absorption spectra reported recently by Luo *et al.*[9]

High-resolution XPS spectra were measured in a Scienta ESCA 300 spectrometer at NCESS, Daresbury Laboratory, U.K. and soft XAS/XES experiments were performed at the undulator beamline X1B at the National Synchrotron Light Source, Brookhaven National Laboratory.[10]

Calculations were performed using DFT (Refs. 11 and

a)Electronic mail: david.payne@chem.ox.ac.uk.
b)Electronic mail: lpiper@binghamton.edu.

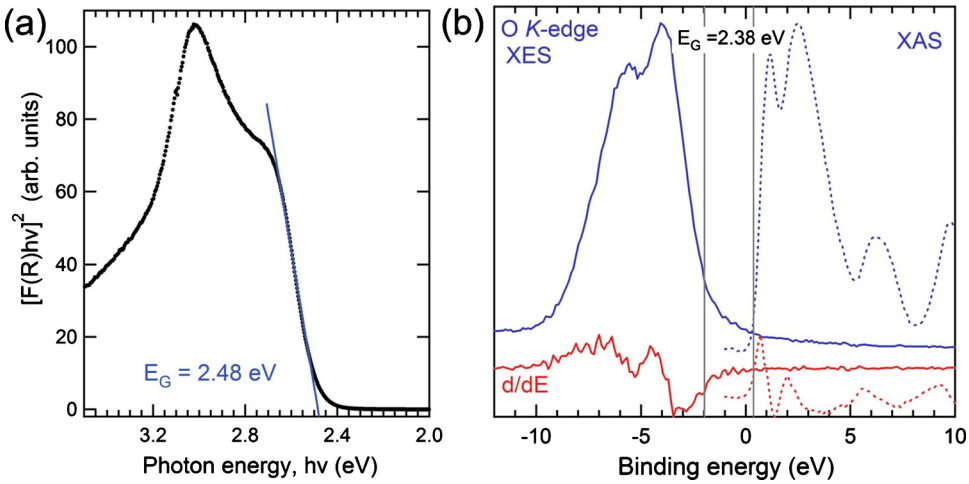

FIG. 1. (Color online) (a) The diffuse reflectance spectrum of monoclinic $BiVO_4$. A linear extrapolation to the baseline was used to determine the onset of the conduction band (i.e., E_g). (b) The O *K*-edge XES (solid line) and core-hole corrected TEY-mode O *K*-edge XAS (dashed line) spectra of $BiVO_4$. The derivatives (solid and dashed lines) are plotted underneath, along with the energetic separation between their edges (i.e., E_g).

12) as implemented in the VASP (Refs. 13 and 14) code. Three dimensional periodic boundary conditions were used to approximate an infinite solid.[15] Exchange-correlation effects were described through the generalized gradient approximation, within the Perdew–Burke–Ernzerhof[16] formalism. Further details are reported elsewhere.[5]

A combination of the O *K*-edge XAS and XES can be employed to deduce the bulk fundamental gap between the occupied (XES) and unoccupied (XAS) states of metal oxides (i.e., E_g). The core-hole final state of the XAS results in a shift to lower photon energies, which in the case of ZnO was found to be ~1 eV,[17] thereby reducing the apparent separation of the XES/XAS. Although less significant for O *K*-edge absorption than for the transition metal *L*-edges, it still needs to be accounted for. In this case, we have employed *resonant* XES in a similar manner as previously considered for ZnO.[17] Resonant XES (RXES) can be viewed as a scattering process where the final state includes an electron in the conduction band and a hole in the VB but no core hole. By exciting at the O *K*-edge onset, we were able to determine the energetic difference due to the core-hole shift to be 1.067 eV from analyzing the elastic peak energy in the RXES. Applying this correction, and using the second derivative of the onsets, as shown in Fig. 1(b), we obtained a value of 2.38 eV in good agreement with our optical measurements.

Figure 2(a) displays the partial fluorescent yield (PFY) XAS of the V $L_{3,2}$-edge and O *K*-edge regions. The relative intensity difference between the regions reflects the Auger to fluorescent yield ratio for the two edges while the features in the O *K*-edge TEY mode are sharper due to the difference in resolution between the techniques. The O *K*-edge excitation was chosen to be well-above threshold for normal emission of the O 2*p* pDOS. Direct comparison with the occupied calculated pDOS and our emission spectra is plotted in Fig. 2(b). For fairer comparison, we have subtracted the Shirley background and considered the cross-section weighted (DFT) pDOS (i.e., cross-section × pDOS/number of electrons per orbital). The O *K*-edge and V L_α-edge XES were shifted by their respective core-hole binding energies. As a result, all the experimental data are referenced to the Fermi level. As such, it is seen that the Fermi energy in $BiVO_4$ lies closer to the CBM than the VBM (~0.3 eV below the CBM). This is in good agreement with Yin *et al.*,[18] who predict a doping stabilization level 0.3 eV below the CBM for an oxygen poor material.

The spectrum in Fig. 3 confirms significant hybridization between the V 3*d* and O 2*p* states at 3 eV below the VBM as predicted by the calculations. Unlike the photoelectron spectroscopy, XES measurements do not suffer from surface effects and so this cannot be attributed to any V^{4+} contribution at the surface. This can be further illustrated by identifying the absence of a corresponding peak in the XES above the calculated VBM position (i.e., 2.2 eV). The feature in the VB-XPS is attributed to reduced vanadium at the surface,

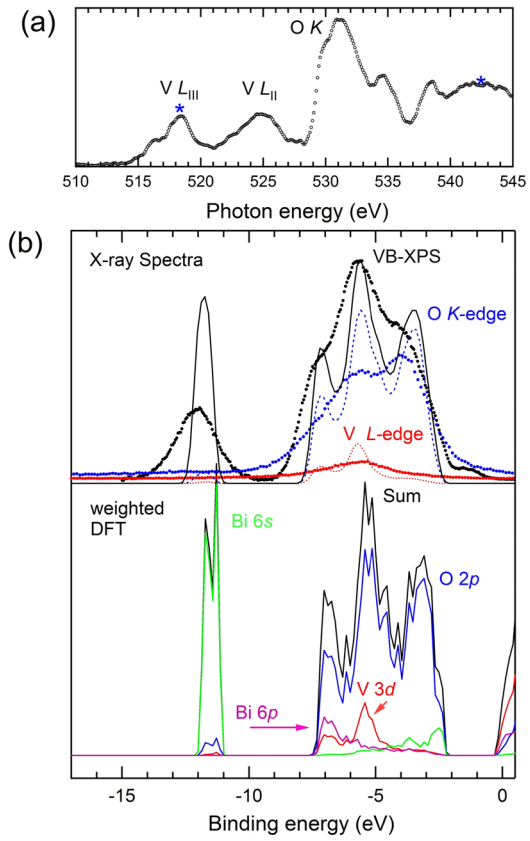

FIG. 2. (Color online) (a) The V $L_{3,2}$- and O *K*-edge PFY-mode XAS. The excitation energies for the emission processes are identified by blue asterisks. (b) The experimental XPS, and core-level shifted XES are plotted with the calculated pDOS underneath (cross-sectioned weighted). Also shown alongside the experimental data are the corresponding Gaussian broadened (full width half maximum=0.4 eV) DOS (dashed lines).

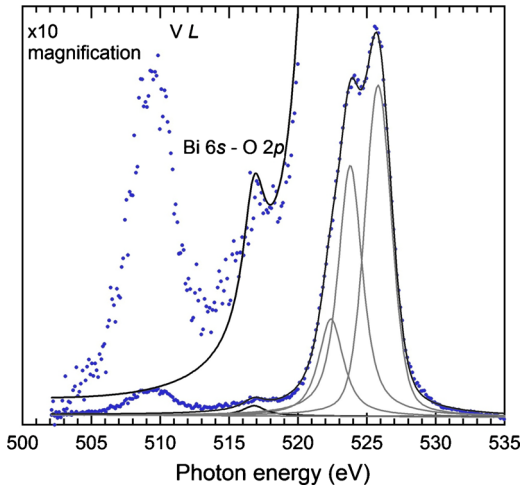

FIG. 3. (Color online) The above threshold O *K*-edge XES (blue filled circles) as a function of photon energy. The V L_α at ~510 eV, also excited by the excitation of the O *K*-edge, is identified. The O 2*p* region has been curve-fitted using four Voigt functions to mimic the four peaks in the calculated O 2*p* pDOS. The inset displays the magnified region to show the Bi 6*s*–O 2*p* bonding state at ~517 eV.

consistent with the V 2*p* core-level XPS. The peak at ~10 eV below the VBM in the VB-XPS [Fig. 2(b)] is the occupied Bi 6*s* states.[6] The difference in the peak height between the XPS and the weighted DFT is attribute to overestimation of the Bi 6*s* cross-section due to relativistic effects not being fully considered. This overall result is consistent with the RLP model, used to describe Bi_2O_3 (Ref. 6) and the calculated electronic structure.[5]

In the RLP model, significant mixing between Bi 6*s* and O 2*p* states exists giving rise to a filled antibonding state with minority 6*s* character at the top of the VB with a majority 6*s* contribution at the bottom of the VB. In the case of Bi_2O_3, ~80% of the Bi 6*s* electron density is located at these energies, with the remaining contribution to this peak coming from the O 2*p* orbital,[6] consistent with our aforementioned assignment. In order to confirm this further, we have examined the O *K*-edge XES to determine the O 2*p* contribution to this peak. Figure 3 displays the O *K*-edge spectra, which also includes the V L_α-edge emission at ~510 eV. For the excitation energy used here to excite the O *K*-edge, the corresponding V L_β-edge emission peak is suppressed and only contributes at energies at the V L_2-edge absorption peak.[19] This implies that the weak peak at 517 eV is related to the O 2*p* states. Curve-fitting the O *K*-edge in the same manner as described by Payne *et al.* confirms agreement with the predicted energetic position of this peak (i.e., 10.5 eV below the VBM). The O 2*p* contribution ($f_{O\ 2p}$) at this energy was determined by comparing the curve-fitted area ratios (A^{peak} and A^{total}) by

$$f_{O\ 2p} = \frac{(A^{peak}/A^{total})}{(n/p)}, \quad (1)$$

where *n* is the number of metal atoms per formula unit and *p* is the total number of valence electron pairs per formula unit ($BiVO_4$, $n=2$ and $p=26$). This gives an experimental $f_{O\ 2p}$ of 0.206, in excellent agreement with the value of 0.198 from DFT. It also agrees well within the overall trend in $f_{O\ 2p}$ versus group number for the RLP model.[6] This result confirms the validity of using the RLP model to describe $BiVO_4$, specifically the Bi 6*s*-O 2*p* antibonding state derived VBM. As a result, we can assign the fundamental E_g at ~2.4 eV (Fig. 1) as due to transitions between the hybrid Bi 6*s*-O 2*p* orbital and unoccupied V 3*d* states (with significant O 2*p* and Bi 6*s* contributions). Meanwhile, the peak in the diffuse spectrum ~0.5 eV above the onset edge is likely associated with occupied O 2*p* states solely, thus experimentally confirming the original hypothesis of Kudo *et al.*,[2] used to explain the difference between tetragonal and monoclinic $BiVO_4$. Experimental confirmation of the hybrid O 2*p*–Bi 6*s* character of the VBM, adds further credence to the claims by Walsh *et al.*,[5] of the symmetric light masses for both holes and electrons within this compound.

To conclude, we have used a combination of x-ray spectroscopy and DFT to investigate the electronic structure of $BiVO_4$. Our results confirmed both the predicted direct band gap of 2.48 eV and Bi 6*s*–O 2*p* derived VBM. They also highlight the suitability of using combinations of nd^0 and ns^2 cations in more complex oxides to develop PEC materials.

The NSLS is supported by the U.S. Department of Energy, Office of Science, Office of Basic Energy Sciences, under Contract No. DE-AC02-98CH10886. D.J.P. acknowledges the support by the U.K. Royal Society (Research Grant No. RG080399) and the award of a Junior Research Fellowship by Christ Church, University of Oxford. L.F.J.P. acknowledges support from the Faculty/Student Research Support Program at the NSLS, and start-up funds from Binghamton University. The Boston University program is supported in part by the Department of Energy under Contract No. DE-FG02-98ER45680. The NCESS facility at Daresbury Laboratory is supported by EPSRC under Grant No. EP-E025722-1.

[1]A. Fujishima and K. Honda, Nature (London) **238**, 37 (1972).
[2]A. Kudo, K. Omori, and H. Katol, J. Am. Chem. Soc. **121**, 11459 (1999).
[3]A. Kudo, MRS Bull. **36**, 37 (2011).
[4]Z. Yi, J. Ye, N. Kikugawa, T. Kako, S. Ouyang, H. Stuart-Williams, H. Yang, J. Cao, W. Luo, Z. Li, Y. Liu, and R. L. Withers, Nature Mater. **9**, 559 (2010).
[5]A. Walsh, Y. Yan, M. N. Huda, M. M. Al-Jassim, and S.-H. Wei, Chem. Mater. **21**, 547 (2009).
[6]D. J. Payne, R. G. Egdell, A. Walsh, G. W. Watson, J. Guo, P.-A. Glans, T. Learmonth, and K. E. Smith, Phys. Rev. Lett. **96**, 157403 (2006).
[7]A. Walsh, J. L. F. D. Silva, S.-H. Wei, C. Korber, A. Klein, L. F. J. Piper, A. DeMasi, K. E. Smith, G. Panaccione, P. Torelli, D. J. Payne, A. Bourlange, and R. G. Egdell, Phys. Rev. Lett. **100**, 167402 (2008).
[8]L. F. J. Piper, A. DeMasi, S. W. Cho, A. R. H. Preston, J. Laverock, K. E. Smith, K. G. West, J. W. Lu, and S. A. Wolf, Phys. Rev. B **82**, 235103 (2010).
[9]H. Luo, A. H. Mueller, T. M. McCleskey, A. K. Burrell, E. Bauer, and Q. X. Jia, J. Phys. Chem. C **112**, 6099 (2008).
[10]See supplementary material at http://dx.doi.org/10.1063/1.3593012 for a full description of these experimental techniques.
[11]P. Hohenberg and W. Kohn, Phys. Rev. **136**, B864 (1964).
[12]W. Kohn and L. J. Sham, Phys. Rev. **140**, A1133 (1965).
[13]G. Kresse and J. Furthmuller, Comput. Mater. Sci. **6**, 15 (1996).
[14]G. Kresse and J. Furthmuller, Phys. Rev. B **54**, 11169 (1996).
[15]M. C. Payne, M. P. Teter, D. C. Allan, T. A. Arias, and J. D. Joannopoulos, Rev. Mod. Phys. **64**, 1045 (1992).
[16]J. P. Perdew, K. Burke, and M. Ernzerhof, Phys. Rev. Lett. **77**, 3865 (1996).
[17]A. R. H. Preston, B. J. Ruck, L. F. J. Piper, A. DeMasi, K. E. Smith, A. Schleife, F. Fuchs, F. Bechstedt, J. Chai, and S. M. Durbin, Phys. Rev. B **78**, 155114 (2008).
[18]W.-J. Yin, S.-H. Wei, M. M. Al-Jassim, J. Turner, and Y. Yan, Phys. Rev. B **83**, 155102 (2011).
[19]O. Y. Khyzhun, T. Strunskus, W. Grunert, and C. Woll, J. Electron Spectrosc. Relat. Phenom. **149**, 45 (2005).